Electronic Supplementary Information

Functional nanoscale metal-organic particles synthesized from a new vinylimidazole-based polymeric ligand and dysprosium ion

Jian Cui,[a,†] Guangfa Zhang,[a,†] Lanxia Xin,[a] Peng Yun,[b] Yehai Yan,[a,*] Feng Su[b,*]

[a] Key Lab of Rubber-plastics, Ministry of Education/Shandong Provincial Key Lab of Rubber-plastics, School of Polymer Science and Engineering, Qingdao University of Science and Technology, Qingdao 266042, China

[b] Department of pharmaceutics, School of Chemical Engineering, Qingdao University of Science and Technology, Qingdao 266042, China

[†] These authors contributed equally.

[*] Corresponding authors. E-mail address: yhyan@qust.edu.cn (Y. Yan); qdkd.sufeng@hotmail.com (F. Su)

Table S1 Effect of shear rate on particle size of $\mathbf{S_2}$.

Shear rate [s^{-1}]	0	10^3	5×10^3	10^4
Particle size [nm]	34.8 ± 3.6	34.6 ± 3.8	34.6 ± 2.7	34.3 ± 2.0

Taking $\mathbf{S_2}$ ethanol colloid (50 mg mL^{-1}) as a typical example, stability of $\mathbf{S_N}$ colloids against shear was studied in terms of the particle size. For this, a Silverson L5M homogenizer was used to generate high-speed shear by a closely spaced rotor/stator combination. Shear rate ($\dot{\gamma}$) is defined as $\dot{\gamma} \approx \pi ND / \Delta R$, where N, D, and ΔR are the rotor speed, rotor diameter (32 mm), and rotor-stator gap (~100 μm), respectively.[1] After being sheared at a certain rate for 20 min and left standing for 2 h, the top 3/4 liquid was carefully drawn out for DLS measurement to determine the particle size.

Note: In the whole shearing process, the beaker containing $\mathbf{S_2}$ colloid is sealed by polyethylene pliofilm and placed in an icy water bath to prevent the evaporation of ethanol.

Table S2 Effect of dilution or enrichment on stability of $\mathbf{S_2}$ ethanol colloid.

Concentration of $\mathbf{S_2}$ ethanol dispersion [mg mL^{-1}]	1	10	50	65	75
Concentration of centrifugal supernatant [mg mL^{-1}]*	1	10	50	65	69

*Centrifugation condition: 1,000 rpm (110 g of relative centrifugation force)/15 min

Taking $\mathbf{S_2}$ ethanol colloid (50 mg mL^{-1}) as a typical example, stability of $\mathbf{S_N}$ colloids against dilution or enrichment was explored in terms of the colloid concentration. For this, a set of dispersions with desired concentrations were firstly prepared from $\mathbf{S_2}$ colloid (50 mg mL^{-1}) by addition or evaporation of a certain amount of ethanol. After sonication (Elmasonic E30H: 40W/37 kHz/1 min), these dispersions were centrifuged at 1,000 rpm for 15 min to accelerate the deposition process of $\mathbf{S_2}$ particles. Then, the top 2/3 fraction of the centrifugal supernatant ($\mathbf{CS_{1000}}$) was carefully suctioned out for concentration measurement through a so-called weighting method.

Weighting method: A 10 mL portion of $\mathbf{CS_{1000}}$ was added into a centrifugal tube with the known weight of $\boldsymbol{W_1}$. After centrifugation at 12,000 rpm for 1 h, the clear centrifugal supernatant was removed, and the sediment together with centrifugal tube was dried to a constant weight of $\boldsymbol{W_2}$ in a 50 ^{o}C vacuum oven. The concentration of $\mathbf{CS_{1000}}$ is then calculated according to $\boldsymbol{C} = (\boldsymbol{W_2} - \boldsymbol{W_1})/10$ [mg mL^{-1}].

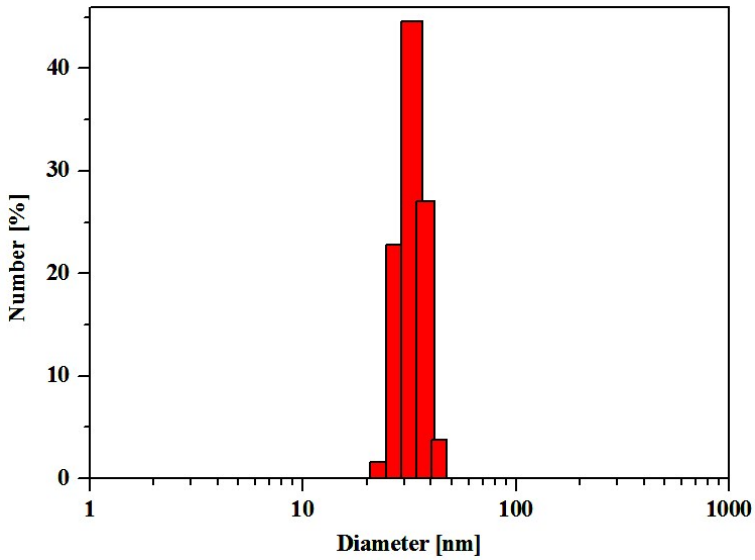

Fig. S1 DLS measurement of $\mathbf{S_2}$.

Through the DLS measurement, average particle size of $\mathbf{S_2}$ was determined to be 34.8 ± 3.6 nm, which agrees well with the TEM determined value of 32.9 ± 7.9 nm.

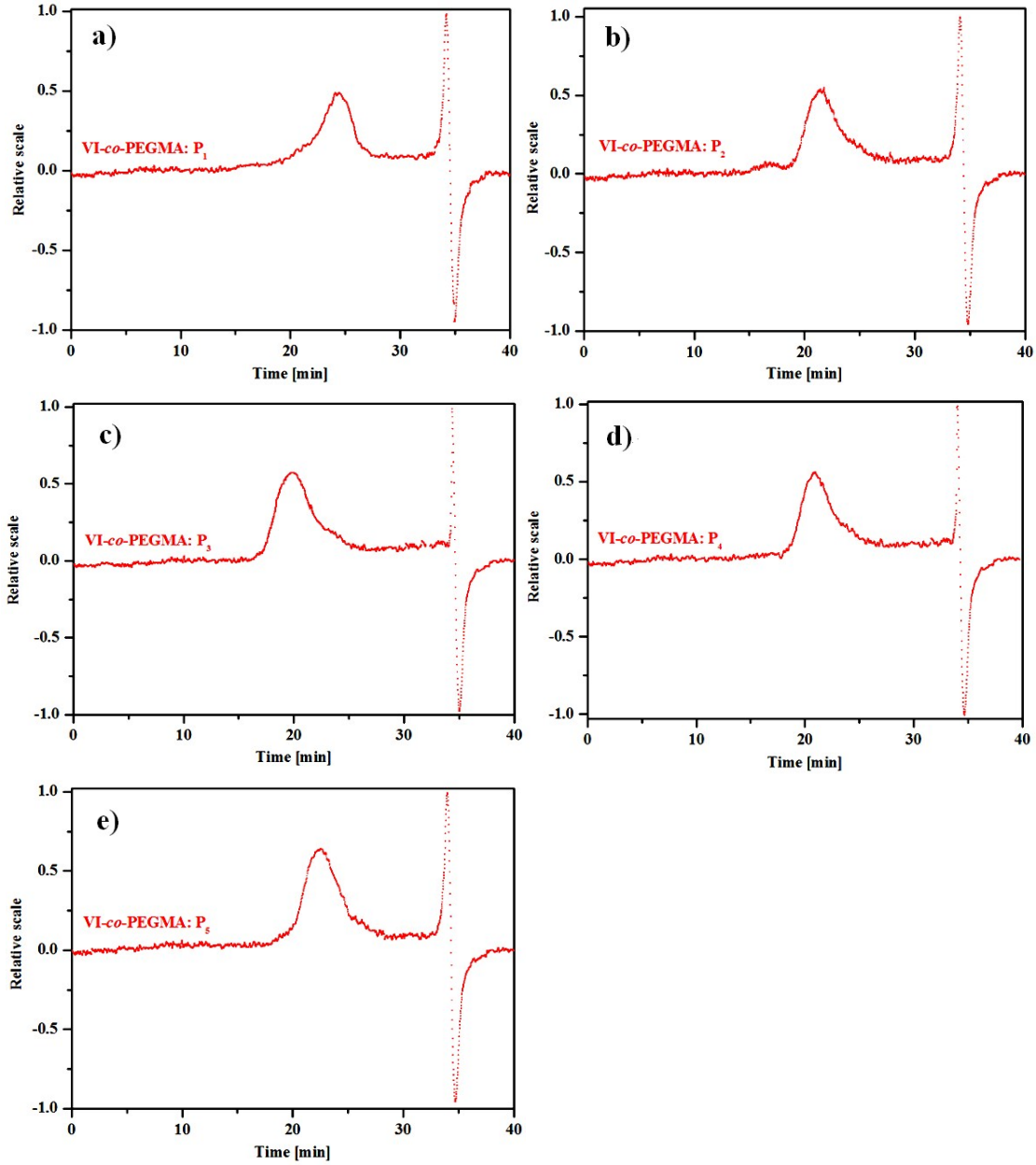

Fig. S2 GPC chromatograms of VI-*co*-PEGMA: a) $\mathbf{P_1}$, b) $\mathbf{P_2}$, c) $\mathbf{P_3}$, d) $\mathbf{P_4}$, and e) $\mathbf{P_5}$.

VI-*co*-PEGMA ($\mathbf{P_N}$, $\boldsymbol{N = 1 \sim 5}$) was dissolved in DMF to produce a clear solution of 2.5 mg mL^{-1}. GPC measurement was then executed on a Waters 1525 separations module with a DAWN HELEOS-II multi-angle (18-angle) light scattering (MALS) detector at room temperature. DMF was employed as an eluent with a flow rate of 1.0 mL min^{-1}. $\overline{M}_n$ and $\overline{M}_w/\overline{M}_n$ of $\mathbf{P_N}$ obtained from the GPC chromatograms (Fig. S2) were summarized in Table 1 (main text).

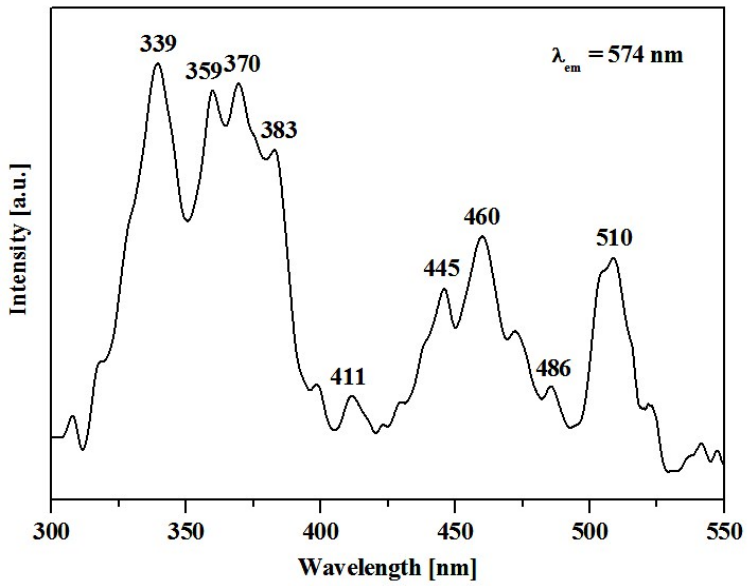

Fig. S3 Fluorescence excitation spectrum of solid state $\mathbf{S_2}$.

A desired volume of $\mathbf{S_2}$ ethanol colloid (50 mg mL^{-1}) was cast on a quartz substrate and fully dried at room temperature for 2 h and then in a 50 ^{o}C vacuum oven for 4 h to produce a thin film with the thickness of 1.1 ± 0.1 μm. The fluorescence excitation spectrum was then recorded under emission at 574 nm. In the subsequent experiments, the maximum excitation wavelength of 510 nm rather than the strongest one of 339 nm was chosen for emission measurements. This is based on two main considerations:

1) Relative to UV light (*e.g.* 339 nm light in this case), the visible light (*e.g.* 510 nm light) causes less harm to biological systems. Therefore, if the 510 nm light can be confirmed to excite strong fluorescence emission, it will be more beneficial for $\mathbf{S_N}$ to develop the optical bio-imaging application.

2) To date, there are already large numbers of literatures dealt with the UV light for excitation of Ln^{3+} chelates, whereas only limited attention was paid to the visible light for excitation.[2-8]

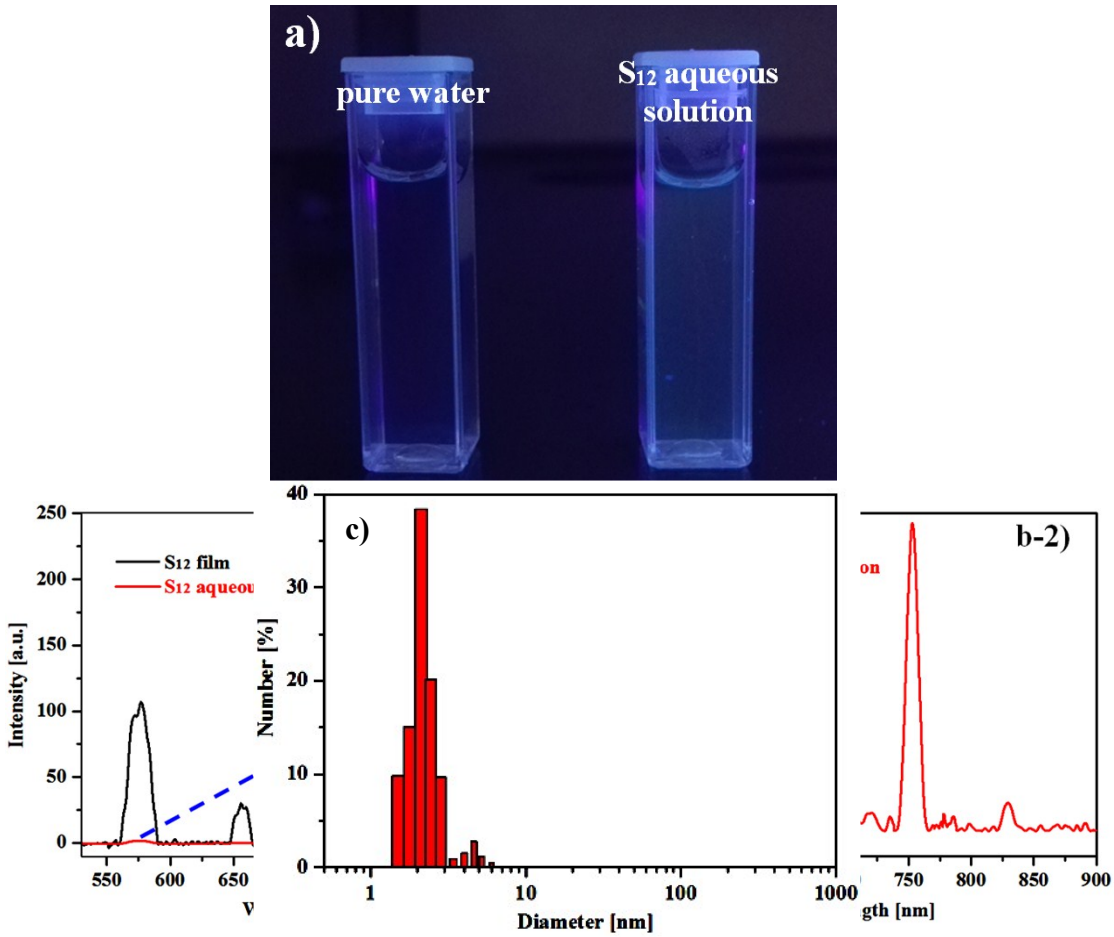

Fig. S4 a) Digital photo of pure water and $\mathbf{S_{12}}$ aqueous solution irradiated by 365 nm UV light, b) fluorescence emission spectra (excited@510 nm) of $\mathbf{S_{12}}$ aqueous solution and $\mathbf{S_{12}}$ film coated on quartz substrate from ethanol colloid, and c) DLS measurement on $\mathbf{S_{12}}$ aqueous solution.

When water was added into the $\mathbf{S_{12}}$ powder, a clear aqueous solution was formed. This solution emits nearly no fluorescence under 365 nm UV light irradiation (Fig. S3a). Further characterization by fluorescent spectroscopy shows that *ca.* 98% of the

fluorescence emission (97.7% for 574 nm emission and 97.5% for 753 nm emission), determined from the emission peak area, is quenched in $\mathbf{S_{12}}$ aqueous solution relative to that of $\mathbf{S_{12}}$ film (Fig. S3b). Meanwhile, the DLS measurement reveals that NPs still exist in $\mathbf{S_{12}}$ aqueous solution but their average size has dramatically decreased to 2.2 ± 0.7 nm (Fig. S3c), compared with 34.9 ± 2.2 nm for as-synthesized $\mathbf{S_{12}}$. These data clearly suggest that most of $\mathbf{S_{12}}$ chelates have been disassembled into the precursors of Dy^{3+} and VI-*co*-PEGMA in water. It is well accepted that fluorescence of lanthanide ions are usually quenched in water, due to the deactivation of excited states through O-H vibration modes of coordinated water molecules.[9] On the other hand, very weak emission of Dy^{3+} observed on $\mathbf{S_{12}}$ aqueous solution (Fig. S3b) reflect the interior hydrophobic environment of surviving NPs.

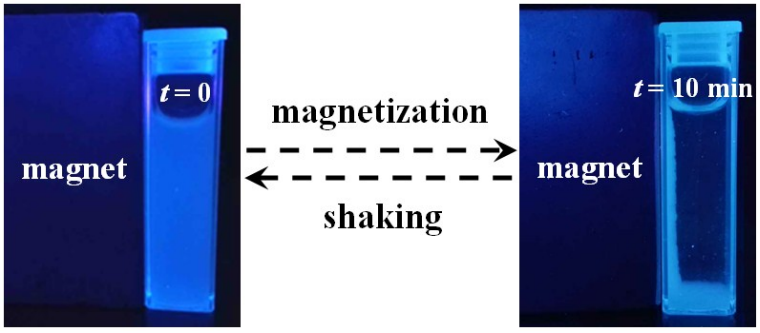

Fig. S5 Digital photo of **S_{12}@silica** aqueous colloid irradiated by 365 nm UV light under an external magnetic field of 0.3 T.

S_{12}@silica can be easily dispersed in water to form a stable aqueous colloid, which emits light blue fluorescence under 365 nm UV light irradiation. Once exerting a 0.3 T magnetic field for 10 min, most of light blue-fluorescent **S_{12}@silica** can be attracted to the side of container facing magnet. By removing the magnet and gently shaking, the collective **S_{12}@silica** readily re-disperse in water.

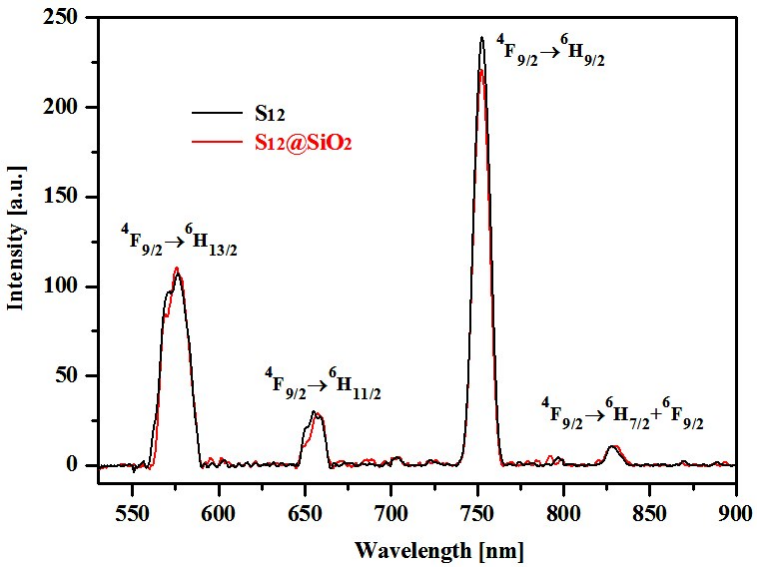

Fig. S6 Fluorescence emission spectra of solid state $\mathbf{S_{12}}$ and $\mathbf{S_{12}}$**@silica**.

The solid state $\mathbf{S_{12}}$ sample (film thickness: 1.0 ± 0.1 μm**)** was prepared by the same process as that of $\mathbf{S_2}$. For preparation of the $\mathbf{S_{12}}$**@silica** sample, a desired volume of $\mathbf{S_{12}}$**@silica** aqueous colloid (25 mg mL^{-1}) was cast on a quartz substrate and fully dried at room temperature for 24 h and then in a 50 °C vacuum oven for 4 h to yield a 1.2 ± 0.1 μm thick film. The fluorescence emission spectra were recorded under excitation at 510 nm. Comparison made between $\mathbf{S_{12}}$ and $\mathbf{S_{12}}$**@silica** shows nearly no changes in position and intensity for the fluorescence emission peaks.

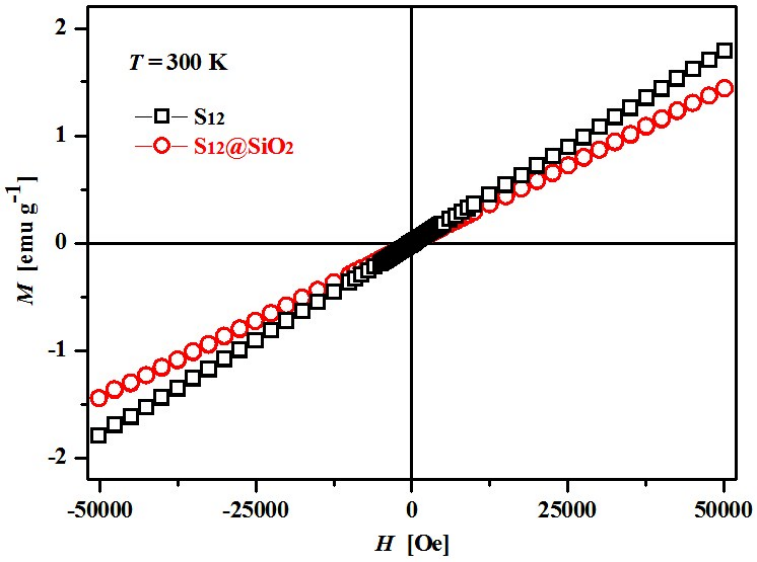

Fig. S7 Hysteresis loop analyses of $\mathbf{S_{12}}$ and $\mathbf{S_{12}@silica}$ at 300 K.

Fitting of $\boldsymbol{M} - \boldsymbol{H}$ plot gives the χ value of 2.9×10^{-5} emu g^{-1} for $\mathbf{S_{12}@silica}$, which shows 19% decrement relative to that of $\mathbf{S_{12}}$ (3.6×10^{-5} emu g^{-1}). This decrease stems from the non-magnetic dilution effect of silica shells in $\mathbf{S_{12}@silica}$.

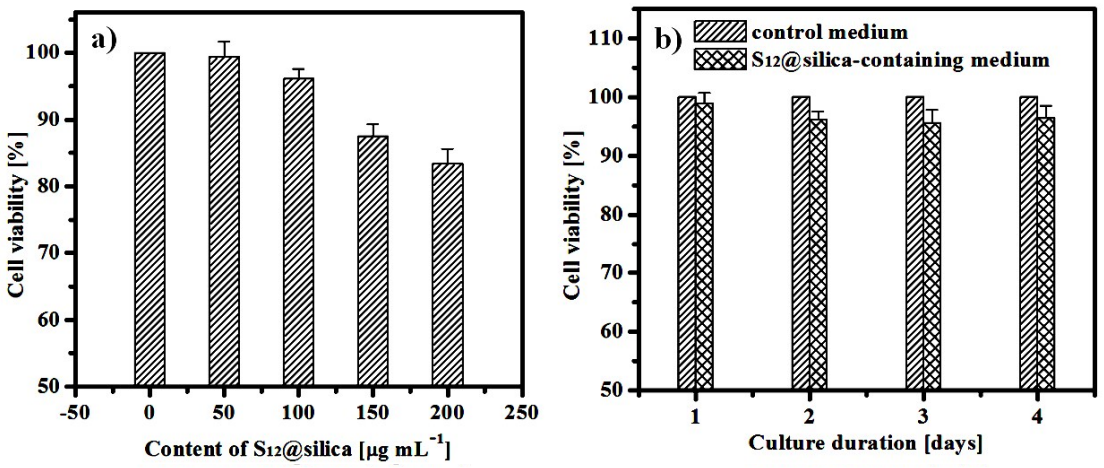

Fig. S8 Cell viability of L929 as a function of a) **S_{12}@silica** content (2 days of culture) and b) culture duration (100 μg mL^{-1} of **S_{12}@silica**).

Under a humidified 37 °C/5% CO_2 environment, L-929 cells (ATCC ccl-1) were seeded in a 96-well plate and incubated at 5000 cells per well in 100 μL of Dulbecco's modified Eagle's medium containing 10% (v/v) fetal bovine serum and 1% (v/v) antibiotics (ThermoFisher Scientific) for 24 h. Subsequently, the culture medium was replaced with isometrical fresh medium containing the desired content of **S_{12}@silica**. To evaluate the effect of **S_{12}@silica** on cell viability, the MTT (methylthiazolyldiphenyltetrazolium bromide, Beyotime) assays were performed. After several days of culture, the cells were aspirated of medium, washed with PBS (100 μL × 5), and incubated in 20 μL of MTT solution (5 mg mL^{-1}) for another 4 h. Thus-formed formazan was dissolved in 150 μL of DMSO, and the absorbance intensity (AI) was measured by a BIO-TEK ELx800 microplate reader at 490 nm. The cell viability (CV) was defined as a percentage of AI to that of control cells. Each CV test was performed in triplicate. Within the content range of 50 ~ 200 μg mL^{-1}, **S_{12}@silica** shows 83.3 ~ 99.4% of CV (Fig. S7a). The effect of culture duration on CV was also studied by fixing the **S_{12}@silica** content at 100 μg mL^{-1}. Over the culture duration, the CV values (95.6 ~ 98.9%) are found very similar with those of the control group (Fig. S7b).

References

1 K. R. Paton, E. Varrla, C. Backes, R. J. Smith, U. Khan, A. O'Neill, et al, *Nat. Mater.*, 2014, **13**, 624-630.

2 N. J. J. Johnson, S. He, S. Diao, E. M. Chan, H. Dai and A. Almutairi, *J. Am. Chem. Soc.*, 2017, **139**, 3275-3282.

3 X. Zhao, S. He and M. C. Tan, *J. Mater. Chem. C*, 2016, **4**, 8349-8372.

4 L. Marciniak, D. Hreniak and W. Strek, *J. Mater. Chem. C*, 2014, **2**, 5704-5708.

5 S. Mohapatra, B. Rajeswaran, A. Chakraborty, A. Sundaresan and T. K. Maji, *Chem. Mater.*, 2013, **25**, 1673-1679.

6 X. J. Zhang, M. A. Ballem, M. Ahren, A. Suska, P. Bergman and K. Uvdal, *J. Am. Chem. Soc.*, 2010, **132**, 10391-10397.

7 R. Nishiyabu, N. Hashimoto, T. Cho, K. Watanabe, T. Yasunaga, A. Endo, K. Kaneko, T. Niidome, M. Murata, C. Adachi, Y. Katayama, M. Hashizume and N. Kimizuka, *J. Am. Chem. Soc.*, 2009, **131**, 2151-2158.

8 B. Mallick, B. Balke, C. Felser and A.-V. Mudring, *Angew. Chem. Int. Ed.*, 2008, **47**, 7635-7638.

9 J.-C. G. Bunzli and C. Piget, *Chem. Soc. Rev.*, 2005, **34**, 1048-1077.